ENC-2022-0404
MAGNETIC REFRIGERATION TECHNOLOGY ASSESSMENT: DESIGN OF A MAGNETIC WINE COOLER

Alan Tihiro Dias Nakashima
Elias Pagnan
Natália Maleski de Sá
Anderson Martins Lorenzoni
Glenda de Melo Luz
Gislaine Hoffmann
Guilherme Fidelis Peixer
Jaime Andrés Lozano Cadena
Jader Riso Barbosa Jr.

POLO – Research Laboratories for Emerging Technologies in Cooling and Thermophysics, Department of Mechanical Engineering, Federal University of Santa Catarina Florianópolis, SC, 88040-900, Brazil
alan.nakashima@polo.ufsc.br
elias.pagnan@polo.ufsc.br
natalia.sa@polo.ufsc.br
anderson.lorenzoni@polo.ufsc.br
glenda.luz@polo.ufsc.br
gislaine@polo.ufsc.br
guilherme.peixer@polo.ufsc.br
jaime@polo.ufsc.br
jrb@polo.ufsc.br

Abstract. *Although our physical understanding of the magnetocaloric effect and its applications has increased substantially in the past few decades, much remains to be done regarding the development and evaluation of magnetic refrigeration prototypes operating in relevant environments. In this sense, the Polomag group aims to develop a compact magnetic refrigeration system capable of controlling the temperature of a 31-bottle wine cooler cabinet between 8 °C and 20 °C for an ambient temperature of 25 °C. A preliminary phase of this research consisted of a detailed performance comparison between a magnetic wine cooler prototype and a commercial vapor-compression system, both operating the same insulated cabinet. Performance metrics from this assessment were used to validate a system-level magnetic refrigeration model able to accurately predict the temperature levels and power consumption of the magnetic device. The model was employed in the second phase of the project, which aims at upgrading the magnetic system into a fully integrated "plug-and-play" magnetocaloric wine cooler as efficient as the conventional system at least. In this work, the design of the second version of the magnetic system and its (expected) thermodynamic performance will be presented. The design methodology was built around the system model and a magnet mass minimization routine. Secondary criteria for the efficiency and size of the magnetic cooling unit were also considered. The resulting system is projected to surpass the thermodynamic performance of the previous vapor compression system for lower temperature spans, however, the size of the magnetic unit is still an issue and it represents a key challenge for the future of the magnetic refrigeration in this particular application.*

Keywords: Magnetic refrigerator, technology assessment, performance evaluation

1. INTRODUCTION

This work stems from the developments achieved in more than a decade of research in magnetic refrigeration (MR) at the POLOMAG group of the Research Laboratories for Emerging Technologies in Cooling and Thermophysics (POLO-UFSC, EMBRAPII unit, INCT-RT unit). Regarding the global scenario, the group was created during the initial stages of

research on MR for room temperature applications, following the work of Brown (1976), who proposed a MR system for operation at room temperature, and the discovery of magnetocaloric materials (MCM) with exceptional cooling properties reported by Pecharsky and Gschneidner Jr. (1997).

The background for the growing interest in the MR technology is the search for solutions to the environmental problems associated with refrigeration systems based on the dominant technology, which is the mechanical vapor compression (VC), also called conventional refrigeration. According to Kitanovski (2020), the energy demand associated with air conditioning and room cooling represents 17% of global energy consumption (International Institute of Refrigeration, 2015), a value which could be tripled by 2050 considering the efficiencies of current systems (International Energy Agency (IEA), 2018). Environmental impacts of the VC technology can be classified into direct and indirect emissions. The first occurs due to the leakage of refrigerant fluids with global warming potential (GWP) and ozone depleting potential (ODP). The second is the indirect emissions of GWP gases by electricity generation activities required by refrigeration systems. In the refrigeration industry, the indirect contribution is about 63% of the total impact, with the remaining 37% due to the leakage of refrigerants into the atmosphere (International Institute of Refrigeration, 2017).

Magnetic refrigeration is a potential alternative for an environmentally cleaner refrigeration due to its operating principle, in which refrigerant fluids are replaced by solid state MCMs subjected to thermomagnetic cycles. Thus, the devices responsible for the compression and expansion in the VC are replaced by sources of magnetic field based on permanent magnets, which do not require a continuous source of energy to generate the field. The thermodynamic work of the cycle is obtained by the relative movement between magnet and MCM, which induces the magnetocaloric effect (MCE), a thermodynamically reversible process where changing the magnitude of the applied magnetic field results in a heat exchange or a temperature variation processes in the material. Therefore, application of solid materials would eliminate direct emissions and the risk of accidents involving the flammability and toxicity of some refrigerants, and the reversibility, combined with the possibility of magnetization work recovery, could reduce energy consumption and indirect emissions.

Nevertheless, the distance between the conception and the achievement of these advantages is still substantial, while new challenges may arise associated to the application of rare earth elements (REE). Researches that carried out preliminary life cycle assessments indicated that the environmental impacts related to the energy consumption of magnetic refrigeration may be lower than that of equivalent compression systems (Aprea *et al.*, 2015, 2018). However, some studies show that impacts would be comparable to or exceed those of VC, mainly due to the extraction of REEs, which constitute both the magnetocaloric materials and the permanent magnets (Monfared *et al.*, 2014; Luglietti *et al.*, 2017). Despite the nomenclature, these elements are not among the rarest, and are found in abundance (Habib and Wenzel, 2014). Currently, the main REEs used in MR research are lanthanum, gadolinium and neodymium (Gauß *et al.*, 2016), and to a lesser extent elements such as yttrium, terbium, holmium, erbium and dysprosium (Kitanovski, 2020; Bez *et al.*, 2020). Regarding the application as refrigerants, the most used elements are gadolinium and lanthanum (Gottschall *et al.*, 2019), whereas for permanent magnets, the most important element, not only for MR but also for other applications in renewable technologies, is neodymium, which makes up the neodymium-iron-boron alloys, NdFeB.

Main challenges in the extraction and mining of REE are the presence of radioactive elements in the minerals extracted for their production (ERECON, 2015), as well as economic factors. Thorium, uranium and its decay products, such as radon and lead, are the main concerns, as their accumulation during processing and inadequate handling of the tailings can cause serious environmental and sanitary problems. The regulation of REE mining activities was one of the reasons for the closure of mines and processing plants in the United States of America and Malaysia, and it also contributed to the reduction of Chinese exports and price rise in the first half of the 2010s (USGS Mineral Resources Program, 2014; Ault *et al.*, 2015; Findeiß, 2016). Another aspect of REE application concerns the balance between supply and demand, which is considered critical for new sustainable technologies (European Comission, 2020). The growth of alternative technologies such as wind power and electric vehicles should contribute to an increase in demand for REEs used in wind generators, motors and batteries, demand which already includes other applications in high technology, such as fluid catalysts and metallurgy (Zhou *et al.*, 2017). In this sense, the work of Habib and Wenzel (2014) focused on the potential bottleneck represented by the production of REE, concluding that demand will exceed production of these materials if rates of production remain at the current level. They also show that recycling can reduce the problem, but only in the medium to long term.

Within the scope of MR, a preliminary risk analysis of gadolinium, lanthanum and neodymium shortages indicated that gadolinium should not be considered a candidate for large-scale applications, while the supply of lanthanum should not be a problem, and that of neodymium would be a bottleneck only in advanced stages of technology penetration due to demand competition from other applications (Gauß *et al.*, 2016). Therefore, reducing the magnet mass of refrigerators can become a critical point. The difference between the expected production to demand relation of different REEs is linked to the balance problem, explained in the work of Binnemans (2014). The problem stems from the fact that the extraction of REE minerals results in an excess of elements such as lanthanum when compared to the amount of neodymium produced. Thus, increasing the demand for this material can generate a large stock of the former, negatively impacting the prices of these elements. The solutions proposed for this problem are the recycling or replacement of critical elements, the reduction of their demand, the exploration of alternative forms of production, or the development of new applications for

the excess materials, such as the MR systems.

Considering the global REE exploration scenario, Brazil was one of the main producers and exporters of REE in the first half of the 20th century, losing its place to the United States of America and then to China (Moraes and Seer, 2018). However, the estimated reserves place the country among the three largest reserves, along China and Vietnam (Agência Nacional De Mineração, 2017). Only recently have REEs aroused government interest due to the economic vulnerability that represents the absence of such resources. The perception that sustainable (such as wind turbines and hybrid vehicles) and strategic (such as oil and communication) technologies are impacted by the availability of REE led to some initiatives (Souza Filho and Serra, 2014). Since 2015, the Government of Minas Gerais, through the Companhia de Desenvolvimento de Minas Gerais (Codemge), has been leading the implementation of a laboratory-factory for magnets and rare-earth alloys, LabFabITR. The facilities will produce NdFeB magnets, used in equipment such as high-efficiency motors, wind turbines, and it will also develop customized solutions directly for the market, providing single batches, prototypes or new products[1].

In this context, the developments carried out at POLOMAG are favorably aligned with the research in magnetic refrigeration and exploration of REEs, especially in Brazilian territory. Since its creation, the research group has followed a path that has reached the stage of proving the technology in a conceptual prototype closer to what would be the reality of a commercial magnetic refrigerator. The latest developed prototypes are: the magnetocaloric wine cooler of Nakashima *et al.* (2021) and the magnetocaloric air conditioner of Peixer *et al.* (2021). These devices are at the sixth level (demonstration of a high-fidelity prototype operating in a relevant environment) of the TRL technology development scale [2]. One of the main lessons learned by the group so far was the importance of integrating the development in the various research sub-areas, such as research in materials, in auxiliary systems and in the coupling of each component. This integration is critical for describing the current scenario of technology, qualifying the obstacles to development and identifying issues that have not yet been addressed, such as the comparison between the volume and mass of MR systems in relation to conventional technology (De Sá *et al.*, 2021).

Considering the following circumstances: (i) the current state of development of magnetocaloric refrigeration systems and models, (ii) the environmental and economic problems that may arise from the extraction, processing and application of REEs, and (iii) the potential for national mineral exploration, *this work aims to design a new magnetocaloric refrigeration system for the wine cooler of Nakashima* et al. *(2021), by evaluating different system options originated from the combination of candidates for each subsystem of the prototype and determine in which of them the magnetic system would be more advantageous in terms of the minimization of the critical rare earth elements masses, the minimization of the energy consumption and minimization of the volume of the refrigeration system with respect to that of the refrigerated compartment.*

Regarding point (i), a low computational cost model was developed in order to estimate the behavior of a magnetic refrigeration system in steady-state and transient regimes Nakashima *et al.* (2022). The model includes sub-models of all relevant subsystems, which are: the active magnetic regenerator (AMR), which is composed of the MCM arranged in the form of a porous regenerative matrix, the magnetic circuit (MC) based on NdFeB permanent magnets, the heat exchangers (HEX) and fans, and the hydraulic circuit (HC), which is responsible for the circulation of an aqueous solution that transfers heat between the external and refrigerated environments. The models were used in an optimization routine for the design and selection of components for the new version of the wine cooler. The optimization objectives were outlined according to circumstances (ii). The first objective was to reduce the mass of REE used in the system, more specifically the mass of NdFeB, a material with greater projected demand and more critical in terms of availability than the MCMs considered in the work, which are LaFeSi alloys. Furthermore, the authors assumed that lower NdFeB masses would result in lower social and environmental footprints. The other objectives of the optimization routine were pursued after defining the smallest amount of NdFeB. They are: increasing energy efficiency, aiming to reduce the contribution of MR to indirect emissions of GWP gases; and reducing the size of the system, assuming that an excessive volume of the refrigeration unit would be prohibitive for the technology. The routine main restrictions are the cooling capacity at the operation point, the availability of materials, equipment limitations and the validity range of the models. Design variables include the type and geometry of the AMRs and the magnetic circuit, the geometry of the heat exchangers, the fan power consumption, and the pump and valve options for the hydraulic circuit. Aiming the exploration in the national territory (circumstance (iii)), components considered for the design procedure were restricted to models easily obtainable in the country, with the exception of the MCMs, which are in the initial stages of development in national production.

2. METHODOLOGY

The steps in the conceptual design of the second version of the magnetic wine cooler will be presented in this section. They include: the definition of system requirements; presentation of the main features of each subsystem candidate, as well as their restrictions on performance and operation; and the design and optimization routine of the system.

---

[1]Adapted from http://labfabitr.com.br/sobre/labfabitr/
[2]Available at: www.nasa.gov/pdf/458490main_TRL_Definitions.pdf

2.1 System Requirements and Cabinet

The starting point of the second version of the magnetic wine cooler design is the results achieved by the first version and its comparison with the performance of the mechanical vapor compression system. For simplicity, the magnetic systems will be called, MR1 and MR2, while the original VC system will be called VC1. A detailed video explaining the operation of the first prototype is available online[3].

The work of De Sá (2020) showed that the MR1 system reached about 60% of the thermodynamic efficiency of the VC1 version when operating the same refrigerated cabinet, presenting an 85% higher consumption under the same temperature conditions of 25 °C in the external environment and 12 °C in the cabinet. Moreover, in addition to the results for a cabinet temperature of 12 °C, Fig. 1 (a) presents a comparison of the results achieved by MR1 and VC1 in terms of second-law efficiency as a function of the temperature reached in the cabinet. One of the main conclusions derived from this analysis is the divergent behavior of the greatest efficiency points. While the efficiency of the VC1 increases, that of the MR1 drops drastically with the cabinet temperature. This deterioration of the thermodynamic performance occurs due to the increase in the requirements of cycle frequency, flow rate and power consumption, which doubles for the system to reach temperatures 2 °C lower. In contrast, the VC1 system power consumption increases only 35% for the system to stabilize at a temperature 4 °C lower.
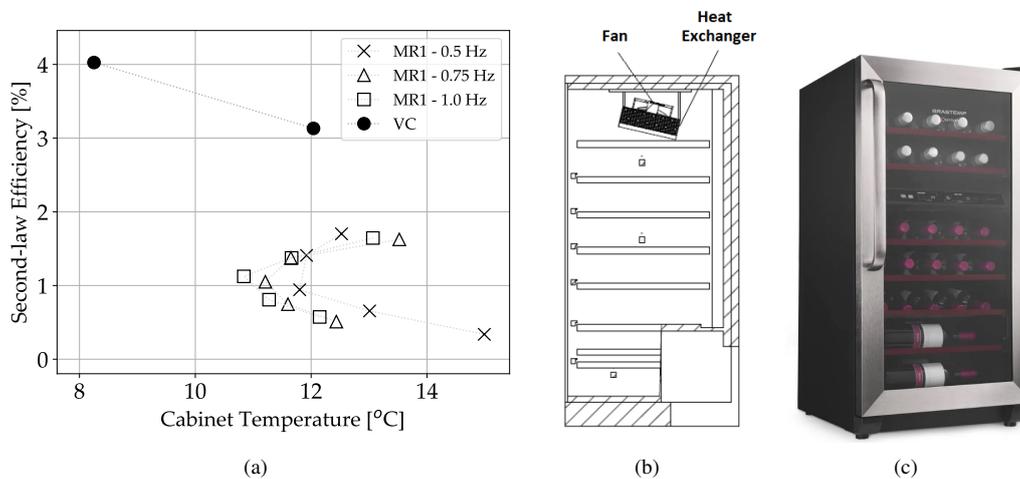

Figure 1. (a) Comparison between the thermodynamic performance of the MR1 and VC1 as a function of the cabinet temperature. (b) the schematic diagram of the cabinet interior and (c) a picture of the cabinet. Adapted from (De Sá, 2020).

In this sense, the MR2 wine cooler design aimed at expanding the operating range of the first version and achieving efficiencies closer to those obtained by conventional technology. Thus, the following specifications were defined: *achieve a cabinet temperature of 8 °C to 12 °C for an ambient temperature of 25 °C with a second-law efficiency greater than 2%.*

The cabinet considered in the project is the same used in the work of De Sá (2020). It has a total volume of 150 l, and its walls have the following constitution: a *liner* composed of high-impact polystyrene (HIPS), a thermal insulation composed of expanded polyurethane with cyclopentane (PU C-Pentane) and an external steel plate. The overall thermal conductance was experimentally evaluated according to De Sá (2020), being equal to 1.75 W K^{-1}. This value defines most of the thermal load requirement that must be absorbed by the refrigeration system. For the temperature difference between environments, equivalent to 17 °C, the minimum capacity that the system must provide is 29.75 W, plus the power consumed by the fan installed inside the cabinet. This power parcel ranged from 1 to 12 W, depending on the fan model selected. Fig. 1 (b) and (c) show an schematic diagram of the cabinet interior as well as its picture, respectively.

2.2 Active Magnetic Regenerators and Magnetic Circuit

The AMRs considered in the project are trapezoidal housings filled with spheroidal particles of LaFeSi alloys. Their particle diameter was 0.75 mm on average, and the porosity of the beds was estimated as 0.38. Fig. 2 shows the arrangement and flow direction in the AMRs, as well as the main features of the magnetic circuit, which is described in the next section. The set of regenerators is represented by a disk divided into 4 or 8 individual beds. Flow occurs in the axial direction, and the length of the regenerator, defined in the flow direction, is given as a fraction of the available length of the MC. The width of each AMR is given as a fraction of the total circumference of the disc, minus the thickness of the

---

[3]https://www.youtube.com/watch?v=y56ApAvZDoA

walls separating the beds (2 mm for each bed). Their height is given by the height of the air gap minus the thickness of the AMR stainless steel housing and the air layer between the rotating part of the circuit and the regenerators. The sum of these thicknesses was considered 4 mm.
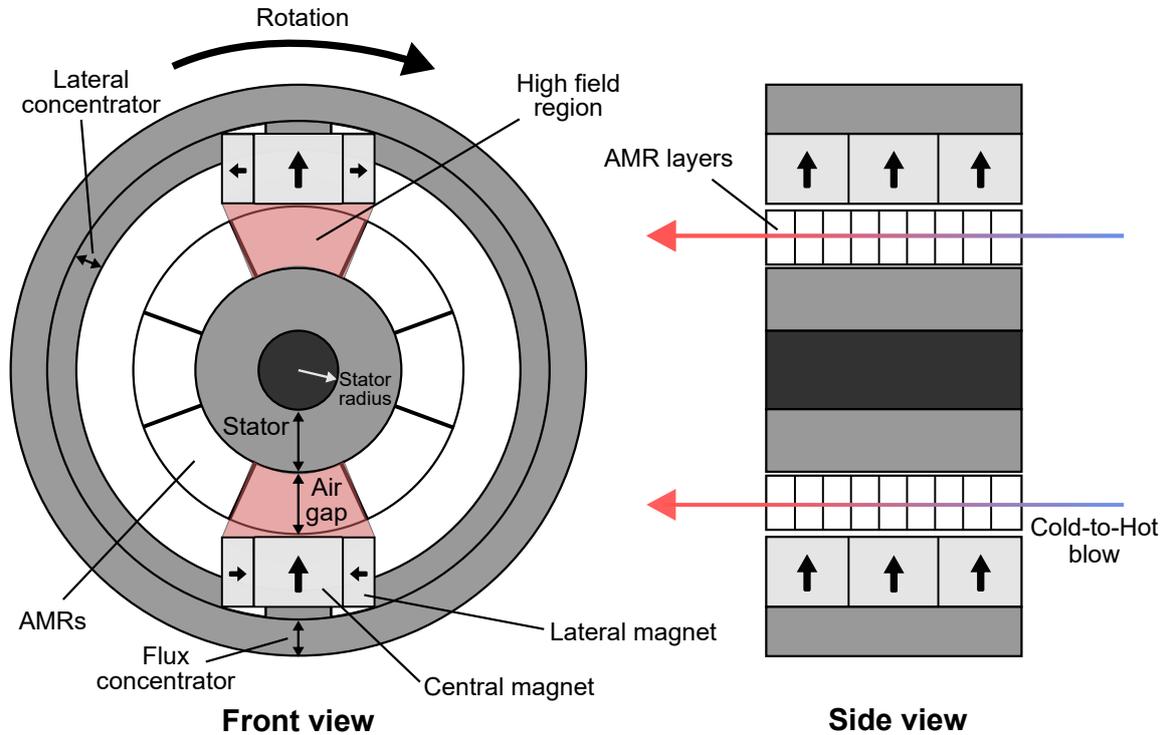

Figure 2. Geometry of the AMR beds and the magnetic circuit.

Design restrictions related to AMRs are related to the utilization factor, whose minimum value was limited to 0.11 due to the validation range of the AMR model. Each AMR bed was divided into 9 layers of LaFeSi alloys, each with a corresponding Curie temperature, which defines the best operation temperature of the material. Thus, the materials were layered in an increasing Curie temperature order, from 4 to 24.9 °C, matching the temperature gradient during the operation of the regenerators. The fraction of each layer was determined by their availability. Hydraulic losses due to the non-sphericity of the particles and thermal losses due to void volumes were considered in the modeling.

The magnetic circuits considered in the project were based on a so-called radial configuration, based on the Halbach cylinder arrangement. In this case, the circuit is composed of an outer rotating cylinder composed of hard and soft magnetic materials. The two regions of hard magnetic material are composed of a central and lateral magnets, and their flux is concentrated into two high induction regions due to the geometry of the flux concentrator and an inner stator, also composed by soft magnetic material. Figure 2 presented its schematic diagram and Tab. 1 the geometric characteristics considered in the design.

Table 1. Parameters of the magnetic circuit

Parameter	Range (mm)	Parameter	Range (mm)
Air gap height (mm)	15 to 40	Stator thickness (mm)	15 to 25
Central magnet height (mm)	25.4 and 50.8	Flux concentrator thickness (mm)	10 to 30
Central magnet width (mm)	50.8	Lateral magnet height (mm)	25.4
Length of the circuit(mm)	50.8 to 152.4	Lateral magnet width (mm)	12.7
Stator radius (mm)	12.7 to 25	Lateral concentrator fraction	40% of the available

In terms of restrictions, the design considered rectangular blocks of NdFeB magnets of commercial dimensions, so the length and height of the hard magnetic material regions assumed continuous values corresponding to the usage of 1 to 3 blocks in the longitudinal direction, and 1 to 2 blocks in the radial direction. The magnet grades presented a remanence of 1.44 T for the central blocks, and 1.21 T for the lateral ones, both with a 1.05 recoil permeability. The maximum magnetic induction allowed for the region of soft magnetic material composed of a S235JR magnetic steel was 1.8 T. The rotating movement of the magnetic circuit responsible for promoting the magnetic induction variation on the AMR beds was defined as a combination of a stepper motor, pulleys and belt. The efficiency of this transmission system was estimated as 80%.

2.3 Heat Exchangers and Hydraulic Circuit

Eight possible arrangements of heat exchangers and hydraulic components were considered in the project, based on the combination of two options for each subsystem: the number of AMRs, the type of the pump in the hydraulic circuit and the mode of operation of the heat exchanger on the hot side (external ambient).

Regarding the hydraulic system, the options are based on the type of pump, which can be unidirectional or oscillatory. The first is represented by a diaphragm pump with maximum flow, pressure difference and efficiency of $250\,\mathrm{l\,h^{-1}}$, 2.8 bar and 30%, respectively. Its characteristic curves were adjusted from a commercially available model. The other type is represented by the piston pump featured in the work of Trevizoli (2015). Restrictions on the maximum rotation for the diaphragm pump and maximum stroke for the piston pump were implemented. Regarding the flow variation profiles, a sinusoidal profile was assumed for the piston pump, as it would be driven by a stepper motor (80% efficiency) and a crank and a connecting rod mechanism. For the diaphragm pump, a trapezoidal profile with a 10% ramp time fraction was assumed. For both options, all the energy supplied to the pump was considered to be transferred to the fluid in the form of either heat or hydraulic power. Fig. 3 (a) and (b) shows photographs of the pumps.

| (a) | PP122.5
      PP92.5
      PP42.5
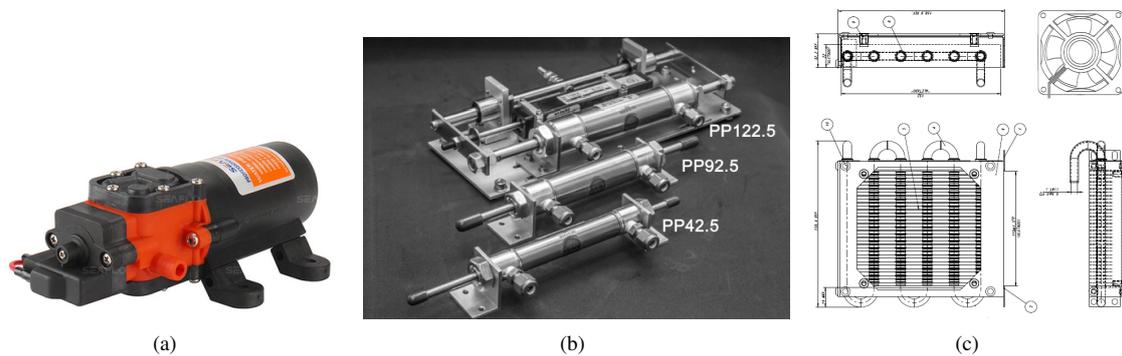   (b) | (c) |

Figure 3. Models for (a) diaphragm pump, (b) piston pump (Trevizoli, 2015) and (c) HEX and fan (Dutra, 2018) considered in the design.

Regardless of the type of pump used, the HC may apply solenoid valves to manage the flow in the two parallel heat exchangers on the hot side, which leads to the options for the hot side heat exchangers operating mode: continuous or oscillatory. The motivation for adopting HEXs operating in oscillatory flow, despite the potential loss of effectiveness, lies in the fact that hydraulic management would not require solenoid valves, thus reducing energy consumption and associated costs. For the cold side (represented by the cabinet), the heat exchanger always operates with continuous flow guaranteed by an arrangement of check valves installed at the inlets and outlets of the AMRs. The type of solenoid valves considered are 4/2 or 3/2, with a nominal energy consumption of 1.5 W, similar to the valves used in the MR1 prototype. Additional pressure losses have been considered in the design, including losses in the check valves, regenerator housing and filters.

The model and geometries of the finned tube HEXs considered in the design are the same used in the MR1 protoype. Their the geometric characteristics and performance can be found in Dutra (2018). A total of six geometries with increasing heat transfer area were considered in the design procedure. Moreover, five axial fan options were also considered, with power consumption ranging from 2 to 12 W, and maximum flow ranging from 67 to 130 CFM. Their operation curve were adjusted from manufacturer data. An example of a finned tube and fan used in this work is shown in Fig. 3 (c).

A total of eight hydraulic circuit schemes were idealized based on the combinations of options for AMRs (4 or 8 beds), pumps (diaphragm, DP, or piston, PP) and hot side heat exchanger mode (continuous, CT, or oscillatory, OC). They are presented in Fig. 4. However, three schemes which are based on the oscillatory HEX were removed from the analysis because they did not present any advantage over the others in terms of reduction in components.

Other considerations were the working fluid, composed of a solution of water and a corrosion inhibitor. Its thermophysical properties were assumed similar to those of the water itself due to the low concentrations of the inhibitor. The blow period fraction of the AMRs was defined as 50%, for the 4 bed cases, and 25% for the 8 bed cases. Moreover, an additional 8 W of power consumption of the system was considered in order to account the electronic system of the prototype.

2.4 Optimization Routine

The optimization routine used in the design of the MR2 prototype was based on the lexicographical method for multi-objective optimization (Arora, 2004). This method is used for problem solving when a hierarchy between objective functions is clearly defined. In such cases, the multi-objective problem is solved as a series of single-objective optimizations, and the results considering each previous objective become constraints for subsequent routines. The advantage of

Cold side (cabinet)

Legend

4 AMRs   8 AMRs

Diaphragm
pump

Piston-
pump

Hot side (external ambient)

AMR
pair

HEX and
fan

DP-CT-4   DP-OC-4   DP-CT-8   DP-OC-8

4/2
valve

3/2
valve

Filter

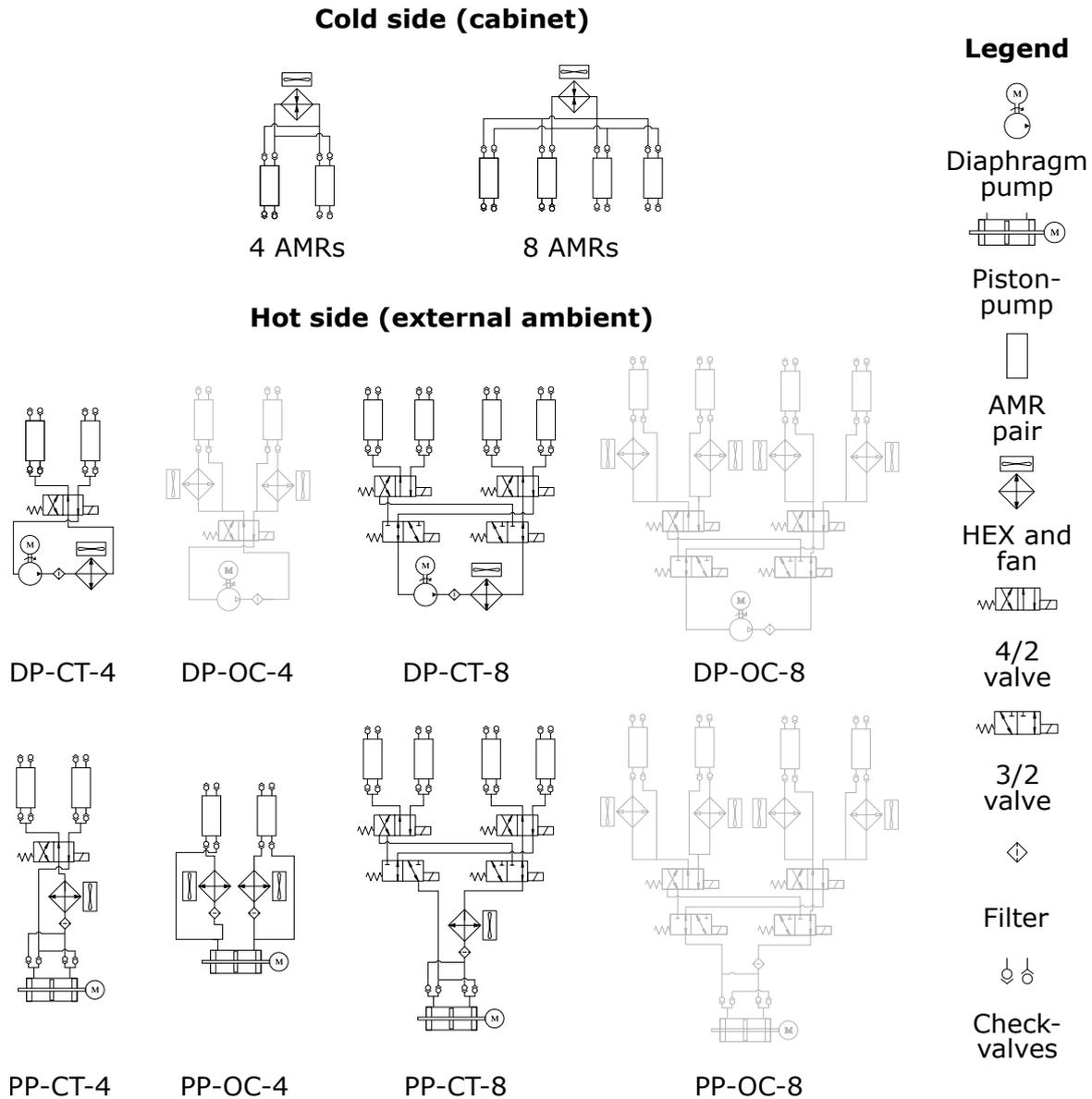PP-CT-4   PP-OC-4   PP-CT-8   PP-OC-8

Check-
valves

Figure 4. Hydraulic schemes considered in the MR2 design. Gray diagrams were removed from the analysis as they did not show improvement potential.

the method is always obtaining a Pareto solution, however its disadvantages include the cost of running multiple single-objective cases in order to get a single solution.

Regarding the MR2 design, the priority order of the objectives was defined as: 1) minimization of the mass of NdFeB; 2) minimization of energy consumption; 3) minimization of refrigeration unit volume. This last point was evaluated through the comparison of the ratio between the useful volume of the refrigerated cabinet and the volume of the cassette of the refrigeration unit achieved by each system. The useful volume was defined as the volume of the refrigerated compartment minus the volume of the heat exchanger and fan assembly installed in the cabinet. The cassette volume was defined as the sum of the volumes required by the MC (1 to 27 l), pump (3.5 l for the piston and 1 l for the diaphragm), solenoid valves (1.27 l each), HEXs (0.36 to 0.72 l each), fans (0.35 l each) and motors (1.56 l each). The volume of accessory components such as fluid reservoir, control unit and others were not considered, as it was assumed that they would not vary significantly between the candidate systems.

The routine proceeded as follows. First, the 5 candidate systems were optimized with the objective of minimizing the mass of NdFeB, and the 2 systems that reached the lowest values of the objective function were selected for the next step. Restrictions of the routine included: the cooling capacity of the system, which must be greater than the thermal load in the cabinet at 8 °C; the maximum heat transfer rate of the hot side HEX defined by its maximum temperature difference, which must be greater than the heat rejection rate of the system; the flow rate, which must be lower than the maximum allowed by the pumps; the regenerator utilization factor, which must be inside the validity range of the AMR model and the

magnetic induction in the soft magnetic material, which must be lower than the saturation value. In the second phase, the systems were optimized in terms of energy consumption with the additional restriction of the maximum allowed NdFeB mass established in the previous step. The two systems that obtained the lowest consumption were classified for the final step, in which their sizes were compared, and the smallest system was selected as the final design. The variables of the mass and power minimization routines, as well as their values ranges are presented in Tab. 2.

Table 2. Range of the design variables. The first eight variables are continuous, whereas the remaining assume discrete values.

Variable	Range
System flow rate	50 to 200 kg h^{-1}
AMR frequency	0.25 to 1 Hz
Air gap height	15 to 35 mm
Lenght fraction of the AMRs with respect to the MC length	50% to 100%
Angular fraction of the AMR with respect to the total available	50% to 100%
Flux concentrator thickness	10 to 30 mm
Stator thickness	15 to 25 mm
Stator radius	12.7 to 25 mm
Maximum temperature difference in the hot HEX	0 to 5 °C
Number of longitudinal magnet blocks	1 to 3
Number of radial magnet blocks	1 to 2
Hot HEX size (n° of rows : fin density in m^{-1})	(1:300), (1:400), (1:500), (2:300), (2:400) or (2:500)
Hot fan power	2, 3, 5, 8 or 12 W
Cold HEX size (n° of rows : fin density in m^{-1})	(1:300), (1:400), (1:500), (2:300), (2:400) or (2:500)
Cold fan power	2, 3, 5, 8 or 12 W

In the optimization routines, the design variables were used as inputs for the magnetic system model detailed in Nakashima *et al.* (2022)[4]. The model is divided into five sub-models: (i) a lumped thermal-hydraulic AMR model, (ii) a semi-analytic model for the magnetic field angular profile, (iii) an empirical model for the pump, (iv) an effectiveness-NTU model for the heat exchangers and lumped thermal model for their oscillatory operation, and (v) a lumped thermal model for the cabinet. The outputs of the model include the steady-state cabinet temperature, power consumption, operation point of the equipment and the dimensions of the system. The solution of the optimization routine was obtained by using a genetic algorithm available in the Pymoo package (Blank and Deb, 2020). Optimization parameters include a population of 500 individuals and 750 offsprings, a mutation and crossover rates of 15% and 30%, respectively, and a convergence criterion of 0,1%, evaluated over the last 200 generations. As the selected system was optimized for a cabinet temperature of 8 °C, a PI temperature controller was also numerically implemented in order to evaluate its performance for a cabinet temperature of 12 °C.

3. RESULTS

The main results of the design procedure are summarized in Tables 3 and 4, which present the performance of the selected system as well as the experimental characterization of the MR1 and VC1 systems for cabinet temperatures of 8 °C and 12 °C, respectively. In terms of hydraulic circuits, the option that achieved the operation point with the lowest NdFeB mass and power consumption was the one designed with the piston-pump, due to its efficiency being higher when compared to the diaphragm pump. The expected values are around 40% for the PP and 20% for the DP. Considering the heat exchanger operation mode, the system based on the oscillatory mode was not able to reach the cabinet temperature specification, thus it is not considered a option for simplifying the hydraulic circuit. Moreover, the number of regenerator beds selected was the highest possible because it allowed for more material to be placed in the circuit and resulted in a better synchronization between magnetic induction variation and flow steps of the refrigeration cycle.

The new system is projected to outperform the previous magnetocaloric wine cooler in NdFeB usage, power consumption and size due to the application of a magnetocaloric material with better thermomagnetic properties (LaFeSi alloys instead of Gd alloys). However, the projected thermodynamic efficiency was 10% lower than that of the conventional technology for a cabinet temperature of 8 °C. Moreover, the size of the refrigeration unit is expected to be four times higher. The predictions are more favorable for a cabinet temperature of 12 °C, where the magnetic system achieves a second-law efficiency 12% higher than that of the conventional system, indicating that the new prototype can be considered for lower temperature spans.

---

[4]with the exception of the magnetic circuit and oscillatory HEX model, which are going to be detailed in a subsequent article.

Table 3. Comparison of the mass, efficiency and volume of candidate systems for the second version (MR2) of the wine cooler prototype. Experimental results of the first version (MR1) and the conventional system (VC1) are also presented. The cabinet temperature is 8 °C for the MR2 and VC1, and 10.8 °C for the MR1 system.

System	NdFeB mass [kg]	Power Consumption [W]	Second-law efficiency [%]	Cooling System Volume [L]
PP-CT-8	6.34	53.63	3.63	21.27
MR1	17.20	118	1.1	43
VC1	9.0^1	42.8	4.0	5^2

[1]Compressor mass

[2]Compressor volume

Table 4. Comparison of the mass, efficiency and volume of candidate systems for the second version (MR2) of the wine cooler prototype. Experimental results of the first version (MR1) and the conventional system (VC1) are also presented. The cabinet temperature is 12 °C.

System	NdFeB mass [kg]	Power Consumption [W]	Second-law efficiency [%]	Cooling System Volume [L]
PP-CT-8	6.34	31.1	3.48	21.27
MR1	17.20	58.5	1.7	43
VC1	9.0^1	31.8	3.1	5^2

[1]Compressor mass

[2]Compressor volume

4. CONCLUSIONS

In this work, a new compact magnetocaloric refrigeration system was designed to operate a wine cooler cabinet and achieve efficiency levels comparable to those of a analogous conventional system with the least amount of REEs. The prototype selected by the means of a optimization routine, which focused on the minimization of NdFeB mass, of the energy consumption and volume of the unit, is expected to outperform previous versions of the wine cooler in terms of power consumption. The gains could be as high as 12% in second-law efficiency when compared to the conventional system for lower temperature spans. However, the magnetocaloric technology is still four times the volume of their VC counterparts and would represent almost 1/4 of the total size of a potential product. One of the reasons for this issue is the lower specific refrigerating effect of solid state. Therefore, research on miniaturization of components or the improvement of thermomagnetic properties are keys to the future of the technology in this application.

5. ACKNOWLEDGEMENTS

6. REFERENCES

Agência Nacional De Mineração, 2017. "Sumário Mineral 2017". Vol. 37. URL https://www.gov.br/anm/pt-br/centrais-de-conteudo/publicacoes/serie-estatisticas-e-economi a-mineral/sumario-mineral/sumariomineral$_2$017.

Aprea, C., Cardillo, G., Greco, A., Maiorino, A. and Masselli, C., 2015. "A comparison between experimental and 2D numerical results of a packed-bed active magnetic regenerator". *Applied Thermal Engineering*, Vol. 90, pp. 376–383.

Aprea, C., Greco, A., Maiorino, A. and Masselli, C., 2018. "The environmental impact of solid-state materials working in an active caloric refrigerator compared to a vapor compression cooler". *International Journal of Heat and Technology*, Vol. 36, No. 4, pp. 1155–1162.

Arora, J., 2004. *Introduction to Optimum Design*. Elsevier Science, Cambridge, Massachusetts.

Ault, T., Krahn, S. and Croff, A., 2015. "Radiological impacts and regulation of rare earth elements in non-nuclear energy production". *Energies*, Vol. 8, No. 3, pp. 2066–2081.

Bez, H.N., Nakashima, A.T., Lang, G.B., de Lima, B.S., Machado, A.J., Lozano, J.A. and Barbosa, J.R., 2020. "Performance Assessment and Layer Fraction Optimization of Gd–Y Multilayer Regenerators for Near Room-Temperature Magnetic Cooling". *International Journal of Air-Conditioning and Refrigeration*, Vol. 28, No. 3, p. 2050027.

Binnemans, K., 2014. "Economics of Rare Earths: the Balance Problem". *ERES2014: 1st European Rare Earth Resources Conference - Milos*, pp. 37–46.

Blank, J. and Deb, K., 2020. "Pymoo: Multi-objective optimization in python". *IEEE Access*, Vol. 8, pp. 89497—89509.

Brown, G.V., 1976. "Magnetic heat pumping near room temperature". *Journal of Applied Physics*, Vol. 47.

De Sá, N.M., 2020. "Thermodynamic comparison of a wine cooler operating with a magnetic prototype and a vapor compression refrigeration system". Undergraduate thesis - Federal University of Santa catarina.

De Sá, N.M., Nakashima, A.T.D., Lozano, J.A. and Jr, J.R.B., 2021. "Thermodynamic Comparison of Magnetocaloric and Vapor Compression Domestic Wine Coolers". *Proceedings in 18th International Refrigeration and Air Conditioning Conference at Purdue*, pp. 1–10.

Dutra, S., 2018. "Avaliação de uma adega doméstica sob a perspectiva de duas tecnologias de refrigeração: compressão mecânica de vapores e refrigeração magnética".

ERECON, 2015. "STRENGTHENING THE EUROPEAN RARE EARTHS SUPPLY-CHAIN Challenges and policy options". p. 102. URL http://ec.europa.eu/DocsRoom/documents/10882/attachments/1/translations.

European Comission, 2020. "Critical Raw Materials Resilience: Charting a Path towards greater Security and Sustainability". *Governance of the World's Mineral Resources*. URL https://eur-lex.europa.eu/legal-content/EN/TXT/PDF/?uri=CELEX:52020DC0474from=EN.

Findeiß, M., 2016. *Effects of radioactive by-products along the extraction of rare earth elements on aquatic and terrestrial organisms*. PhD Thesis - RWTH Aachen University.

Gauß, R., Homm, G. and Gutfleisch, O., 2016. "The Resource Basis of Magnetic Refrigeration". *Journal of Industrial Ecology*, Vol. 21, No. 5, pp. 1291–1300. ISSN 15309290.

Gottschall, T., Skokov, K.P., Fries, M., Taubel, A., Radulov, I., Scheibel, F., Benke, D., Riegg, S. and Gutfleisch, O., 2019. "Making a Cool Choice: The Materials Library of Magnetic Refrigeration". *Advanced Energy Materials*, Vol. 9, No. 34. ISSN 16146840.

Habib, K. and Wenzel, H., 2014. "Exploring rare earths supply constraints for the emerging clean energy technologies and the role of recycling". *Journal of Cleaner Production*, Vol. 84, No. 1, pp. 348–359.

International Energy Agency (IEA), 2018. "The Future of Cooling Opportunities for energy- efficient air conditioning". URL www.iea.org.

International Institute of Refrigeration, 2015. "29th Informatory Note on refrigeration technologies: The role of refrigeration in the global economy". *Iir*, , No. 29, p. 16. ISSN 0042207X. URL https://iifiir.org/en/documents/37047/download.

International Institute of Refrigeration, 2017. "35th Informatory Note on Refrigeration Technologies: The impact of the refrigeration sector on climate change". *IIR Information*, , No. November, p. 17. URL http://www.iifiir.org/.

Kitanovski, A., 2020. "Energy Applications of Magnetocaloric Materials". *Advanced Energy Materials*, Vol. 10, No. 10. ISSN 16146840. doi:10.1002/aenm.201903741.

Luglietti, R., Rosa, P., Pastore, A., Terzi, S. and Taisch, M., 2017. "Life Cycle Assessment Tool Implemented in Household Refrigeration Industry: A Magnetic Cooling Prototype Development". *Procedia Manufacturing*, Vol. 8, No. October 2016, pp. 231–238.

Monfared, B., Furberg, R. and Palm, B., 2014. "Magnetic vs. vapour-compression household refrigerators: A preliminary comparative life cycle assessment". *International Journal of Refrigeration*, Vol. 42, pp. 69–76.

Moraes, L.C.D. and Seer, H.J., 2018. "Terras raras". URL http://recursomineralmg.codemge.com.br/wp-content/uploads/2018/10/TerrasRaras.pdf.

Nakashima, A.T., Peixer, G.F., Lozano, J.A. and Barbosa, J.R., 2022. "A lumped-element magnetic refrigerator model". *Applied Thermal Engineering*, Vol. 204, No. October 2021, p. 117918.

Nakashima, A.T., Fortkamp, F.P., de Sá, N.M., dos Santos, V.M., Hoffmann, G., Peixer, G.F., Dutra, S.L., Ribeiro, M.C., Lozano, J.A. and Barbosa, J.R., 2021. "A magnetic wine cooler prototype". *International Journal of Refrigeration*, Vol. 122, pp. 110–121.

Pecharsky, V.K. and Gschneidner Jr., K.A., 1997. "Giant Magnetocaloric Effect in $Gd_5(Si_2Ge_2)$". *Phys. Rev. Lett.*, Vol. 78, No. 23, pp. 4494–4497. doi:10.1103/PhysRevLett.78.4494.

Peixer, G.F., Vieira, B.P., Fortkamp, F.P., Bez, H.N., Cattelan, L.F.P., Teza, H.F., de Oliveira, M.S., Nakashima, A.T., Lozano, J.A. and Barbosa Jr., J.R., 2021. "Integrated design of a large-scale magnetic refrigerator". *Proceedings in 9th International Conference on Caloric Cooling (THERMAG IX), Maryland, USA*.

Souza Filho, P.C. and Serra, O.A., 2014. "TERRAS RARAS NO BRASIL: HISTÓRICO, PRODUÇÃO E PERSPECTI-VAS". *Química Nova*, Vol. 37, No. 4, pp. 753–760.

Trevizoli, P.V., 2015. "Development of thermal regenerators for magnetic cooling applications".

USGS Mineral Resources Program, 2014. "The Rare-Earth Elements - Vital to Modern Technologies and Lifestyles".

Zhou, B., Li, Z. and Chen, C., 2017. "Global potential of rare earth resources and rare earth demand from clean technologies". *Minerals*, Vol. 7, No. 11. ISSN 2075163X.

7. RESPONSIBILITY NOTICE